



**NATIONAL UNIVERSITY of SINGAPORE**

Department of Mechanical Engineering

# **ME6204 Convective Heat Transfer**

*Term Paper*

**Laminar Flow and Heat Transfer from a Circular Cylinder in  
Cross-flow using by the Lattice-Boltzman Method**

**Lecturer: Professor Arun S. Mujumdar**

**Submitted by**

**WU JIE (g0500388@nus.edu.sg)**

**ZENG HUIMING (g0500326@nus.edu.sg)**

## 1. Introduction

During the last two decades, as an alternative computational fluid dynamics approach, the Lattice Boltzmann method (LBM) has achieved considerable success in fluids engineering. Unlike traditional CFD methods, which are based on the discretization of the macroscopic continuum equations, the LBM is based on the microscopic models, mesoscopic kinetic equations, and the macroscopic dynamics of a fluid is the result of collective behavior of many microscopic particles in the system. The LBM has been proved to recover the Navier-Stokes equation by using the Chapman-Enskog expansion. For more detail, reference [1] can be used.

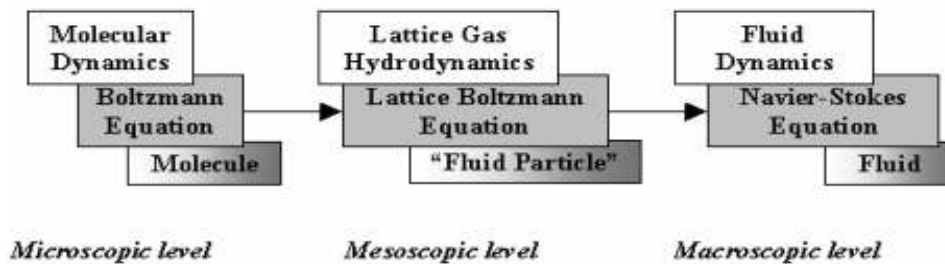


Figure 1.1 Three levels of description of natural phenomena

The fundamental idea behind the LBM is the construction of simplified kinetic models that incorporate the essential physics of microscopic or mesoscopic processes so that the macroscopic averaged properties of the LBM obey the desired macroscopic hydrodynamics. The basic premise of using these simplified kinetic-type method for macroscopic fluid flows is that the macroscopic dynamics of a fluid is the results of the collective behavior of many microscopic particles in the system and the macroscopic dynamics is not sensitive to the underlying details in microscopic physics.

The major advantages of the LBM are its explicit feature of the governing equation — lattice Boltzmann equation, easy for parallel computation and easy for

implementation of complex boundary conditions.

On the other hand, in order to solve the problem about heat transfer, it is necessary to consider the changing of temperature field in the domain. Since there is no very successful thermal model in LBM, we use the macroscopic equation to implement the variation of temperature in the fluid field.

## 2. Methodology

In our simulation, we use the lattice Boltzmann method to simulate the variation of fluid density and velocity, while the changing of temperature field is governed by the macroscopic energy equation.

The standard two-dimensional lattice Boltzmann equation can be written as

$$f_{\alpha}(\mathbf{x} + \mathbf{e}_{\alpha}\delta t, t + \delta t) - f_{\alpha}(\mathbf{x}, t) = -\frac{1}{\tau}(f_{\alpha}(\mathbf{x}, t) - f_{\alpha}^{eq}(\mathbf{x}, t)) \quad (\alpha = 0, 1, 2, \dots, M) \quad (2.1)$$

where  $f_{\alpha}(\mathbf{x}, t)$  is the density distribution function;  $\mathbf{e}_{\alpha}$  is the particle discrete velocity;  $f_{\alpha}^{eq}(\mathbf{x}, t)$  is its corresponding equilibrium distribution function, which depends on the local macroscopic variables  $\rho$  and  $\mathbf{u}$ ;  $\tau$  is the single relaxation time; and  $M$  is the number of particle discrete velocity. Here, we choose the D2Q9 particle model, and so  $M = 8$ . The diagram is sketched in Fig 2.1.

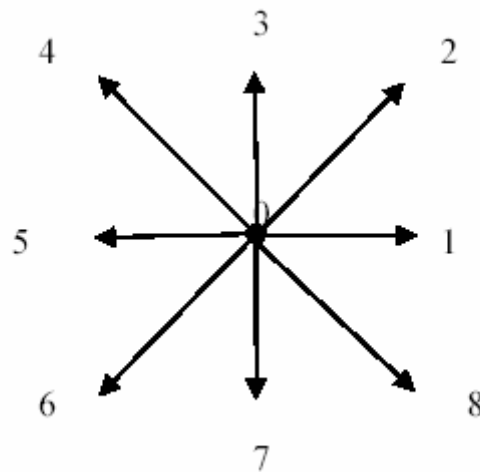


Fig 2.1 D2Q9 model

For the D2Q9 model, the particle discrete velocity is defined as:

$$\mathbf{e}_\alpha = \begin{cases} (0, 0), & \alpha = 0 \\ (\cos[\pi(\alpha-1)/4], \sin[\pi(\alpha-1)/4]), & \alpha = 1, 3, 5, 7 \\ \sqrt{2}(\cos[\pi(\alpha-1)/4], \sin[\pi(\alpha-1)/4]), & \alpha = 2, 4, 6, 8 \end{cases} \quad (2.2)$$

and the equilibrium distribution function is:

$$f_\alpha^{eq} = \omega_\alpha \rho \left[ 1 + 3(\mathbf{e}_\alpha \cdot \mathbf{u}) + \frac{9}{2}(\mathbf{e}_\alpha \cdot \mathbf{u})^2 - \frac{3}{2}(\mathbf{u} \cdot \mathbf{u}) \right] \quad (2.3)$$

where the coefficient  $\omega_\alpha$  is:

$$\omega_\alpha = \begin{cases} 4/9, & \alpha = 0 \\ 1/9, & \alpha = 1, 3, 5, 7 \\ 1/36, & \alpha = 2, 4, 6, 8 \end{cases} \quad (2.4)$$

The macroscopic density  $\rho$  and momentum density  $\rho\mathbf{u}$  can be computed as:

$$\rho = \sum_{\alpha=0}^8 f_\alpha; \quad \rho\mathbf{u} = \sum_{\alpha=1}^8 f_\alpha \mathbf{e}_\alpha \quad (2.5)$$

The equation of state and kinematic viscosity can be defined as:

$$P = \rho c_s^2 \quad (2.6)$$

$$\nu = c_s^2 (\tau - 0.5) \delta t \quad (2.7)$$

where  $c_s^2$  is speed of sound, for D2Q9 model, it is equal to  $1/3$ .

Since the standard lattice Boltzmann equation uses the uniform mesh, in order to extend this method to the non-uniform grid, the modification is necessary. Here, we choose the Taylor series expansion- and Least square based-lattice Boltzmann method.

The two-dimensional governing equation is

$$f_\alpha(x_0, y_0, t + \delta t) = V_{\alpha 1} = \sum_{j=1}^9 a_{\alpha 1, j} g_{\alpha j-1} \quad (2.8)$$

where  $a_{\alpha 1, j}$  is a set of coefficients, which can be computed in advance;  $g_{\alpha j-1}$  is

$$g_{\alpha j-1} = f_\alpha(j-1, t) - \frac{1}{\tau} (f_\alpha(j-1, t) - f_\alpha^{eq}(j-1, t)) \quad j = 1, 2, \dots, 9 \quad (2.9)$$

Obviously, it is a simple algebraic equation and is easy to solve. Details are in reference [2].

The macroscopic energy equation governing temperature changing<sup>[6]</sup> is

$$\frac{\partial T}{\partial t} + \frac{\partial(uT)}{\partial x} + \frac{\partial(vT)}{\partial y} = \frac{\lambda}{\rho c_p} \left( \frac{\partial^2 T}{\partial x^2} + \frac{\partial^2 T}{\partial y^2} \right) \quad (2.10)$$

where  $T$  is temperature;  $u, v$  are the velocities of fluid;  $\lambda$  is the thermal conductivity;  $\rho$  is density;  $c_p$  is fluid specific heat capacity. The term  $\lambda/\rho c_p$  can be written as  $\frac{UD}{\text{Re Pr}}$ , where  $U$  is characteristic velocity;  $D$  is characteristic length, here refers to the diameter of cylinder;  $\text{Re}$  is Reynolds number and  $\text{Pr}$  is Prandtl number.

In order to solve the above equation in the non-uniform grid, we use the coordinate transfer to transfer equation from  $(x, y)$  to  $(\xi, \eta)$ . The final equation is

$$\begin{aligned} \frac{\partial T}{\partial t} + \frac{uy_\eta - vx_\eta}{J} T_\xi + \frac{vx_\xi - ux_\xi}{J} T_\eta = \frac{UD}{\text{Re Pr}} \{ (\alpha T_{\xi\xi} - 2\beta T_{\xi\eta} + \gamma T_{\eta\eta}) / J^2 \\ + [ (\alpha x_{\xi\xi} - 2\beta x_{\xi\eta} + \gamma x_{\eta\eta}) (y_\xi T_\eta - y_\eta T_\xi) + (\alpha y_{\xi\xi} - 2\beta y_{\xi\eta} + \gamma y_{\eta\eta}) (x_\eta T_\xi - x_\xi T_\eta) ] / J^3 \} \end{aligned}$$

where  $\alpha = x_\eta^2 + y_\eta^2$ ;  $\beta = x_\xi x_\eta + y_\xi y_\eta$ ;  $\gamma = x_\xi^2 + y_\xi^2$ ;  $J = x_\xi y_\eta - x_\eta y_\xi$ .

The derivatives in the above equation can be discretized using center difference except for the term of convection. The term of convection can be discretized by windward scheme of third order

$$\left( f \frac{\partial T}{\partial \xi} \right)_{i,j} = \begin{cases} f_{i,j} (T_{i+2,j} - 2T_{i+1,j} + 9T_{i,j} - 10T_{i-1,j} + 2T_{i-2,j}) / 6\Delta\xi & f_{i,j} \geq 0 \\ f_{i,j} (-2T_{i+2,j} + 10T_{i+1,j} - 9T_{i,j} + 2T_{i-1,j} - T_{i-2,j}) / 6\Delta\xi & f_{i,j} < 0 \end{cases}$$

where  $f = \frac{uy_\eta - vx_\eta}{J}$ . And

$$\left( f \frac{\partial T}{\partial \eta} \right)_{i,j} = \begin{cases} f_{i,j} (T_{i+2,j} - 2T_{i+1,j} + 9T_{i,j} - 10T_{i-1,j} + 2T_{i-2,j}) / 6\Delta\eta & f_{i,j} \geq 0 \\ f_{i,j} (-2T_{i+2,j} + 10T_{i+1,j} - 9T_{i,j} + 2T_{i-1,j} - T_{i-2,j}) / 6\Delta\eta & f_{i,j} < 0 \end{cases}$$

where  $f = \frac{vx_\xi - ux_\xi}{J}$ . See reference [8].

### 3. Results and Discussion

In our simulation, we use O-type body fit mesh, as shown in Fig 3.1.

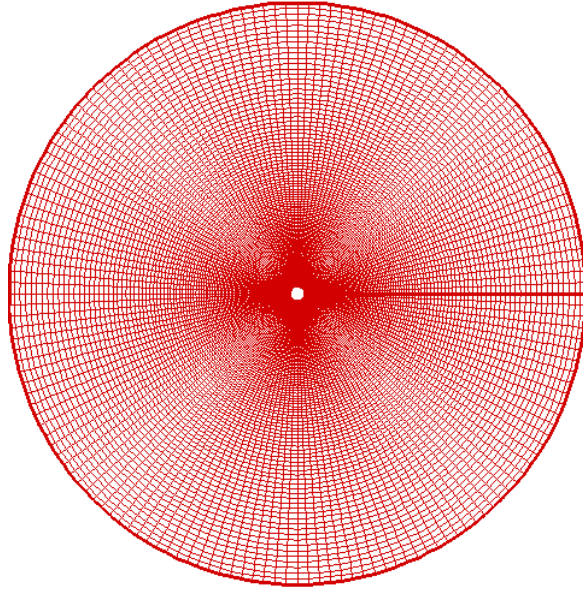


Fig 3.1 O-type body fit grid

Here, the Reynolds number is defined as  $Re = \frac{UD}{\nu}$ , the Prandtl number is  $Pr = \frac{\mu c_p}{\lambda}$ . We set the kinematic viscosity,  $\nu = 0.01$ , free stream velocity  $U = \frac{Re \cdot \nu}{D}$ , and Prandtl number  $Pr = 0.7$  (fluid is air).

**Boundary conditions:**

Initially, the temperature of fluid is  $T_0 = 298.15$  K, the temperature of cylinder is  $KT_w = 473.15$ , the fluid is stationary except that the far field has the free stream velocity.

The density distribution function  $f_\alpha$  in the whole domain is equal to its corresponding equilibrium distribution function,  $f_\alpha^{eq}$ .

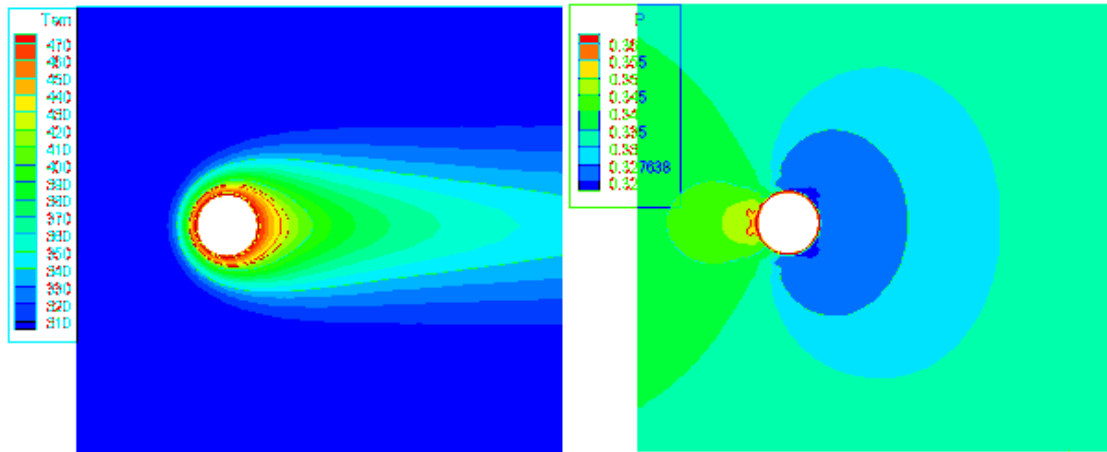
During the process of computation, the temperature of far field and cylinder invariable; at the same time, the velocity of far field constant, equaling to free stream velocity; and the velocity of the surface of cylinder is zero (no-slip condition).

The distribution function  $f_\alpha$  satisfies the bounceback rule at the surface of cylinder; while at the far field, the distribution function  $f_\alpha$  is set to be equal to

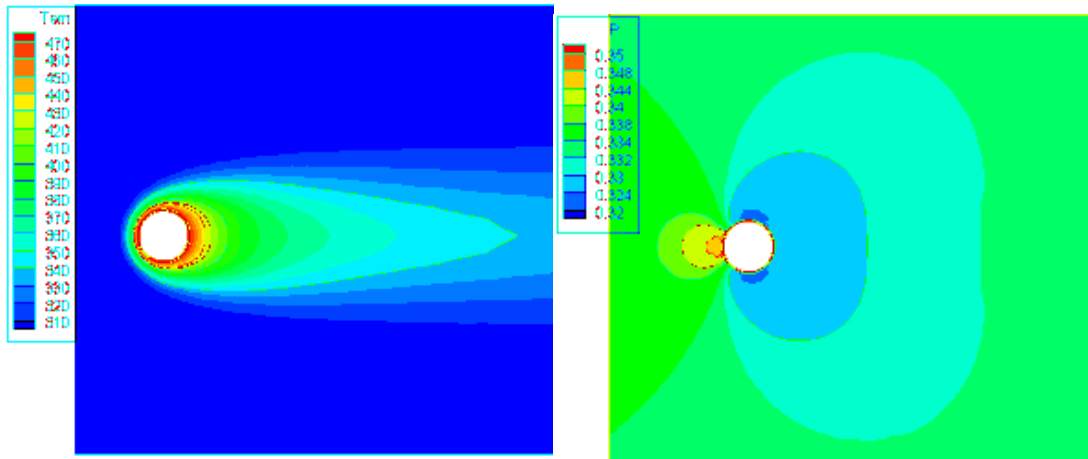
the equilibrium distribution function  $f_{\alpha}^{eq}$ .

### 3.1 Temperature and pressure patterns

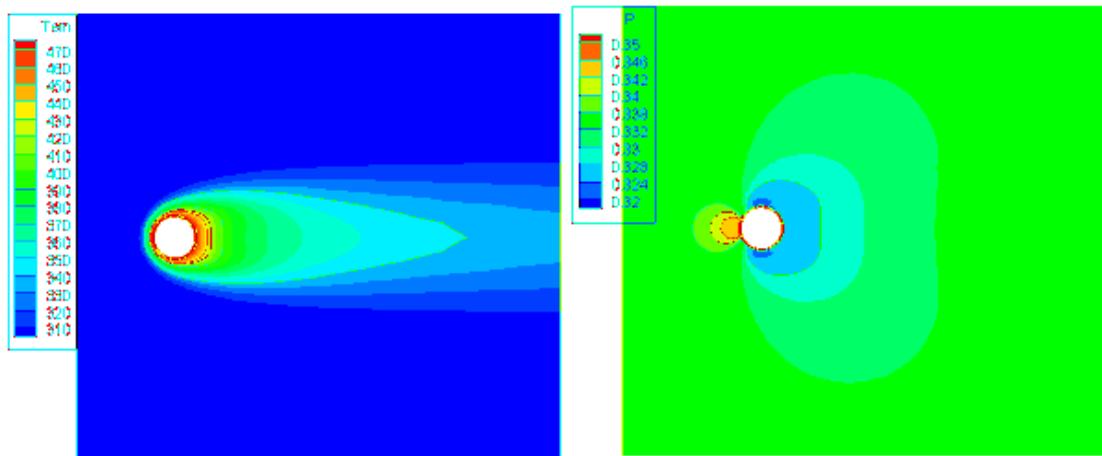
In our simulation, six different Reynolds numbers are selected: 4, 20, 40, 100, 160 and 1000. First, the temperature and pressure patterns are given.



Reynolds number: 4

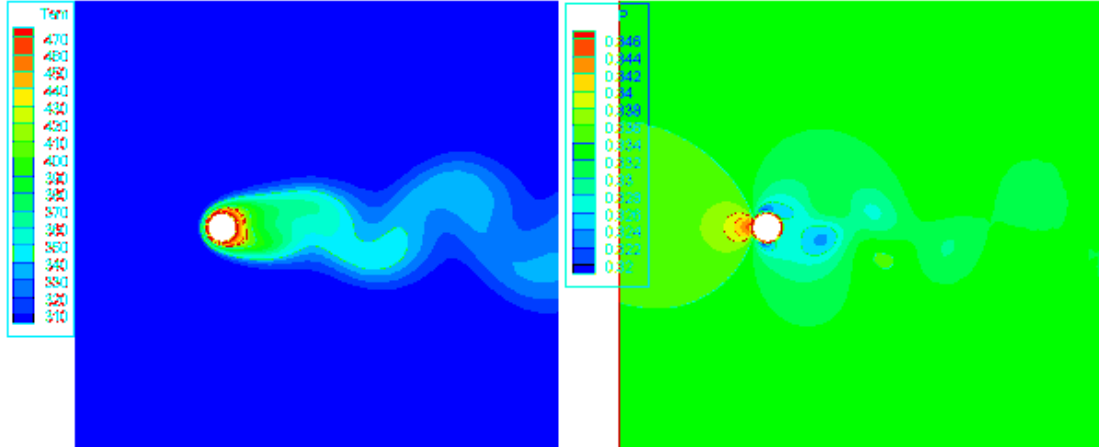


Reynolds number: 20

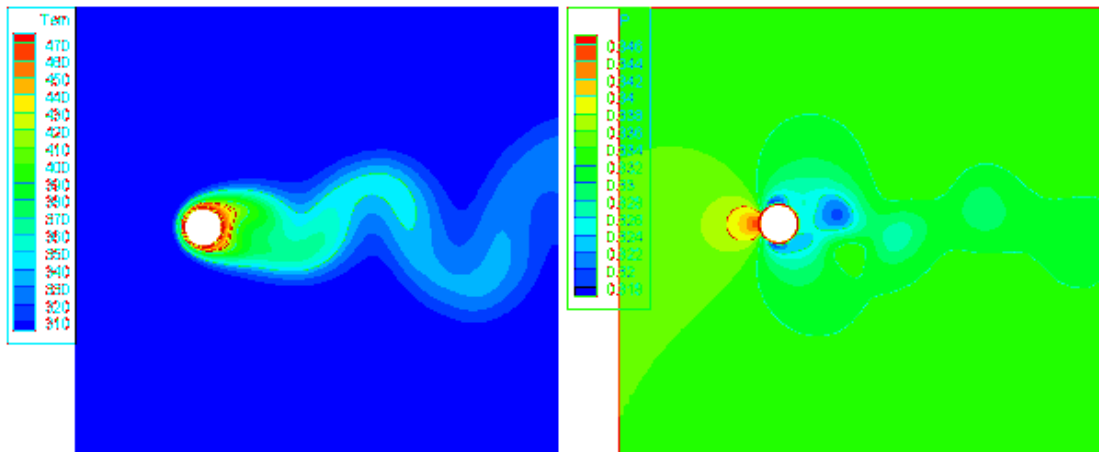


Reynolds number: 40

When the Reynolds number  $1 \leq Re \leq 40$ , the flow is steady, and both upstream and downstream is symmetrical. Therefore, the temperature and pressure patterns are symmetrical as well. At the same time, when the Reynolds number is low ( $Re=4$ ), the thickness of the thermal layer is high. With the increment of Reynolds number, we find that the thickness of thermal layer becomes lower.

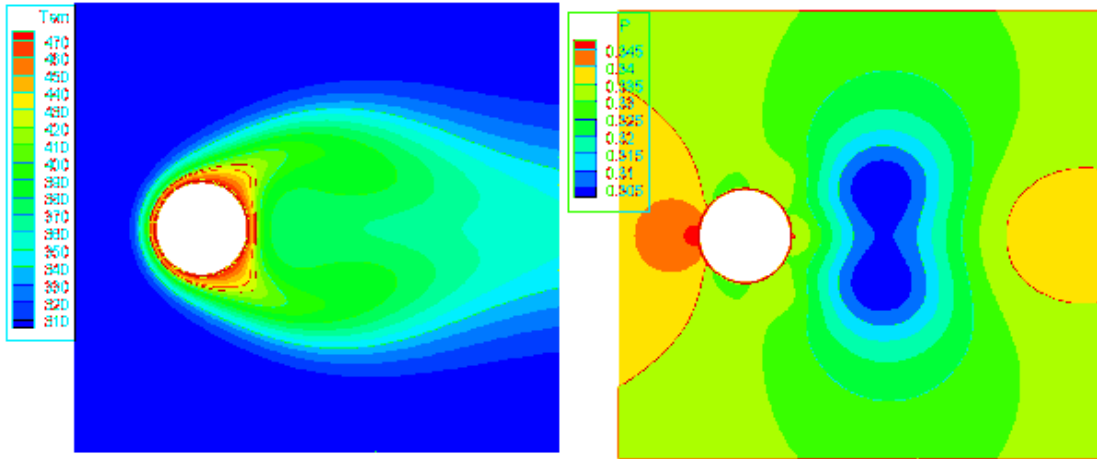


Reynolds number: 100



Reynolds number: 160

When the Reynolds number  $50 \leq Re \leq 160$ , the flow becomes unsteady and periodic. The Karman vortex streets appear and dominate the flow domain finally.

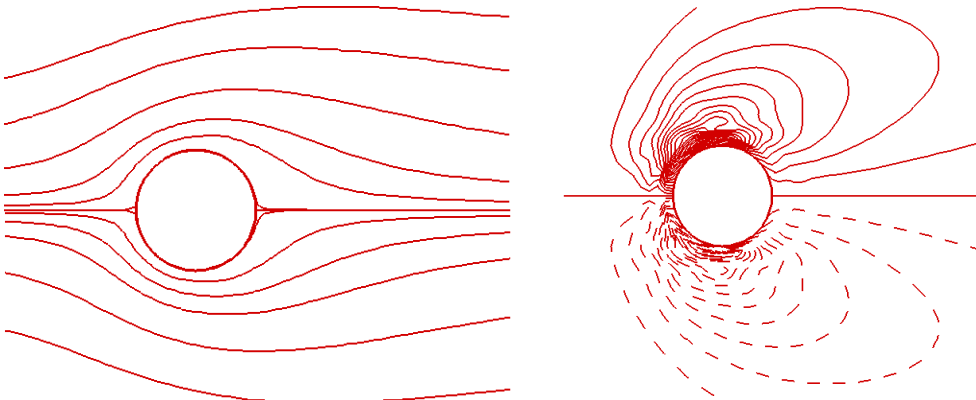


Reynolds number: 1000

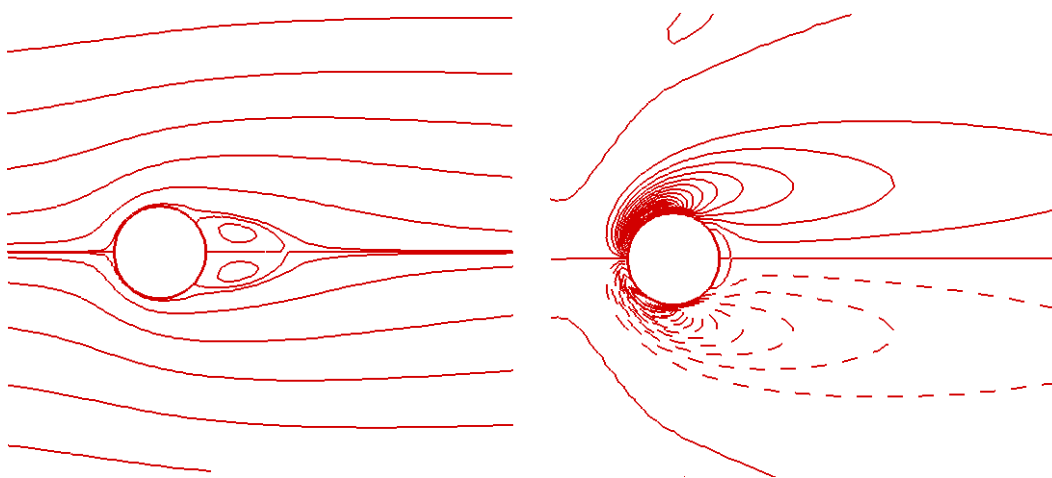
When the Reynolds number  $Re=1000$ , the flow is turbulent.

### 3.2 Streamlines and vorticity contours

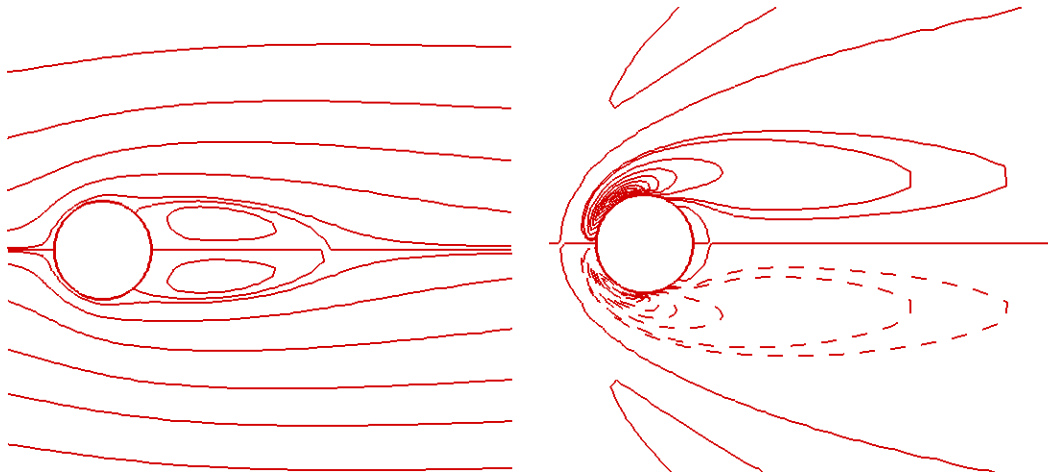
At the same time, we also give the streamlines and vorticity contours at different Reynolds numbers.



Streamline (left) and vorticity contours (right) ( $Re=4$ )

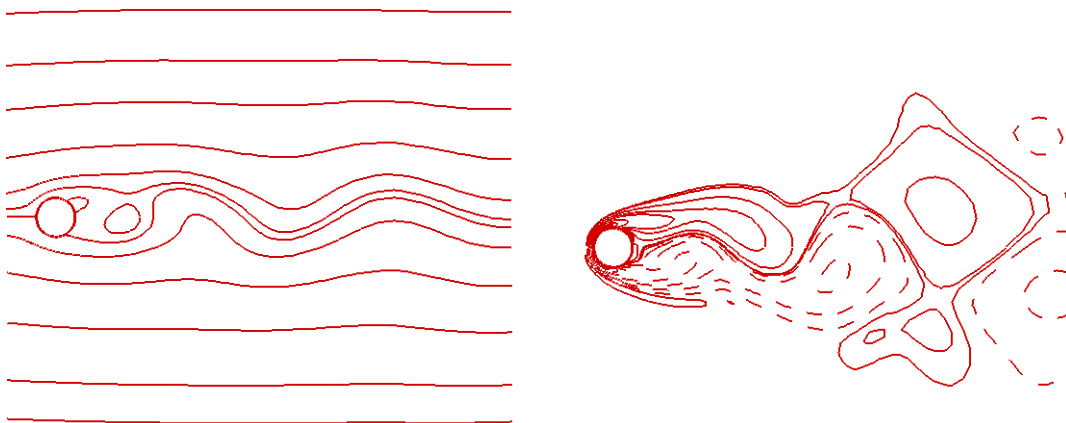


Streamline (left) and vorticity contours (right) ( $Re=20$ )

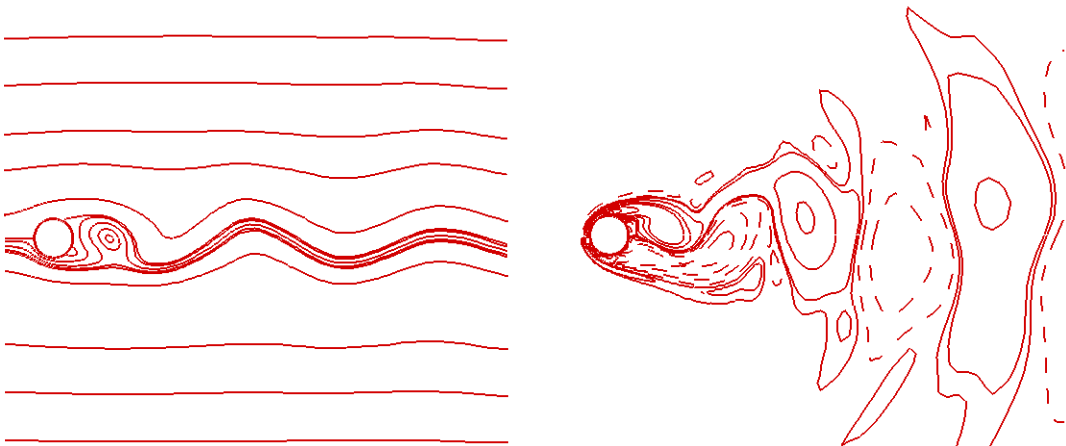


Streamline (left) and vorticity contours (right) (Re=40)

From the above the diagrams, we can find that, when the Reynolds number is low the streamline can keep close to the surface of cylinder. Enhancing the Reynolds number, a couple of vortex would appear behind the cylinder. The size of vortex could increase with the Reynolds number.

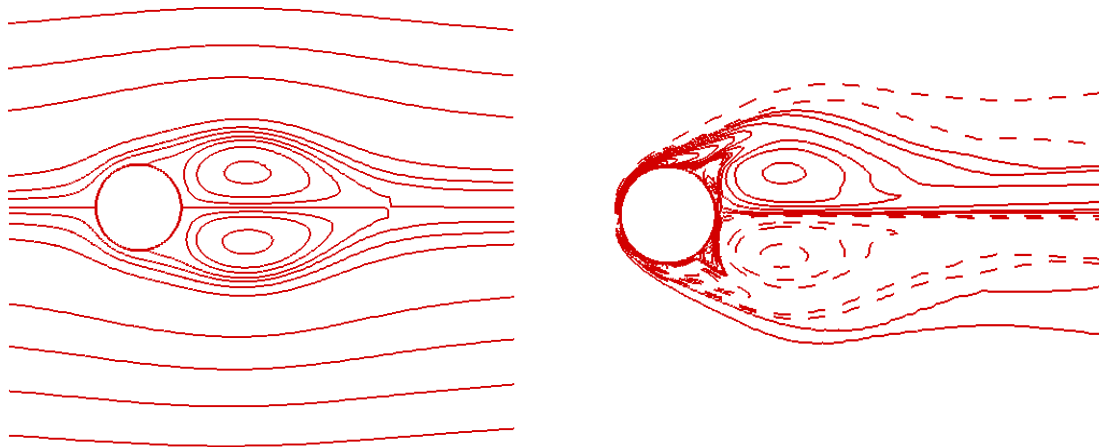


Streamline (left) and vorticity contours (right) (Re=100)



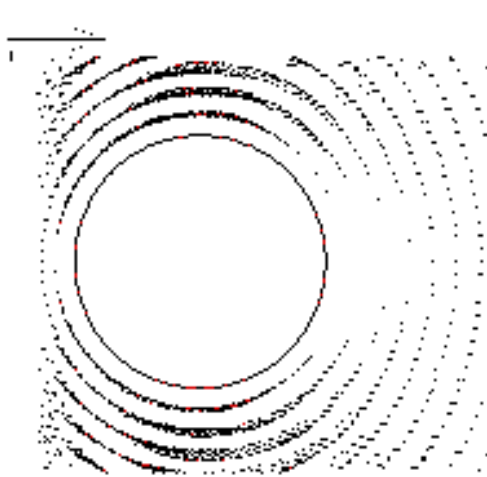
Streamline (left) and vorticity contour (right) (Re=160)

The above figures indicate that the size of Karman vortex street also increases with Reynolds number.

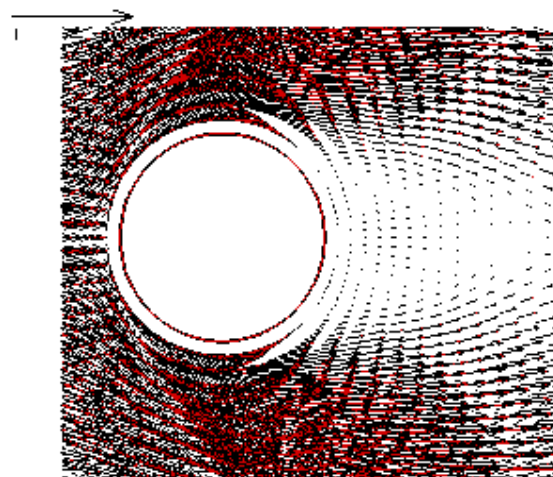


Streamline (left) and vorticity contours (right) (Re=1000)

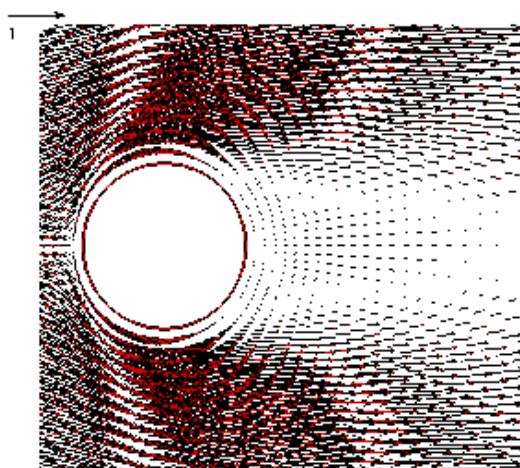
### 3.3 Velocity patterns



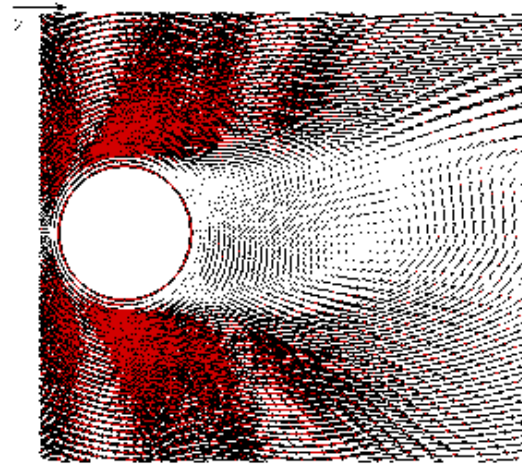
Re=4



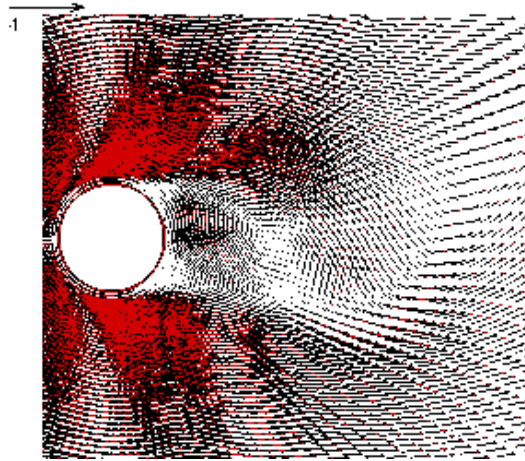
Re=20



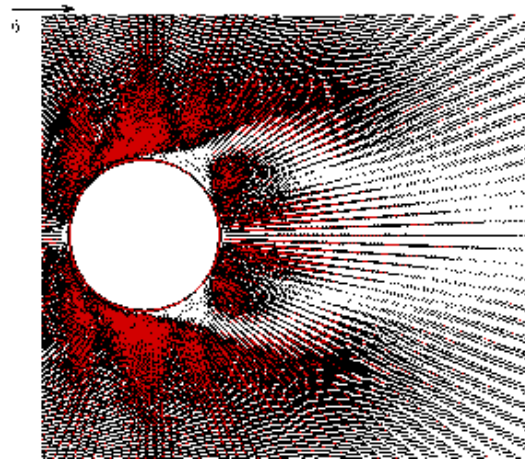
Re=40



Re=100



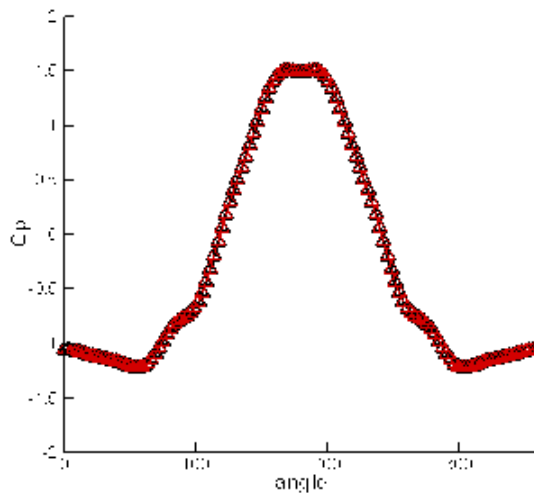
Re=160



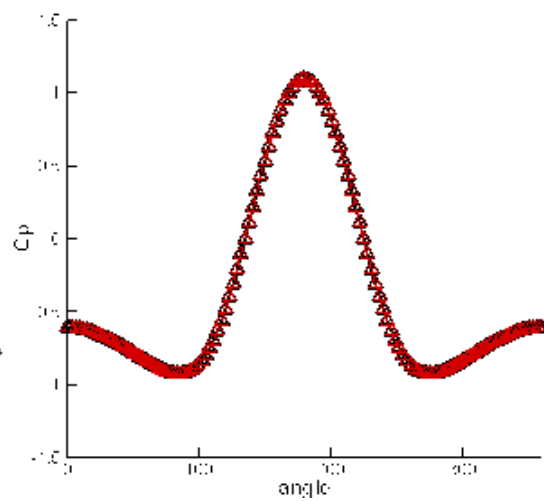
Re=1000

### 3.4 Pressure coefficient along the cylinder

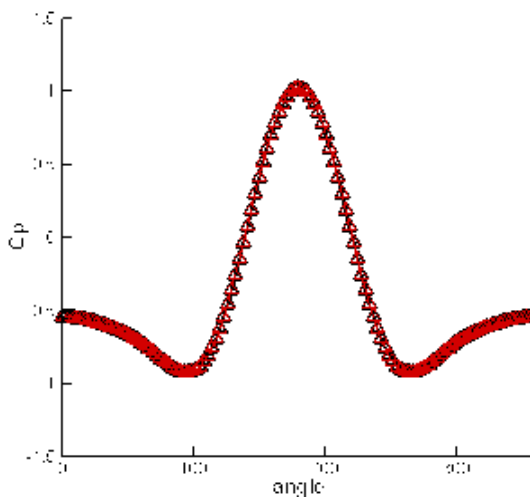
The pressure coefficient along the cylinder is defined as  $C_p = \frac{p - p_0}{\frac{1}{2} \rho_0 U^2}$ .



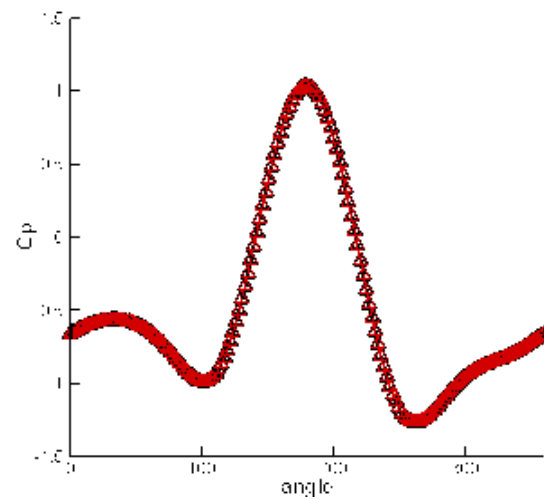
Re=4



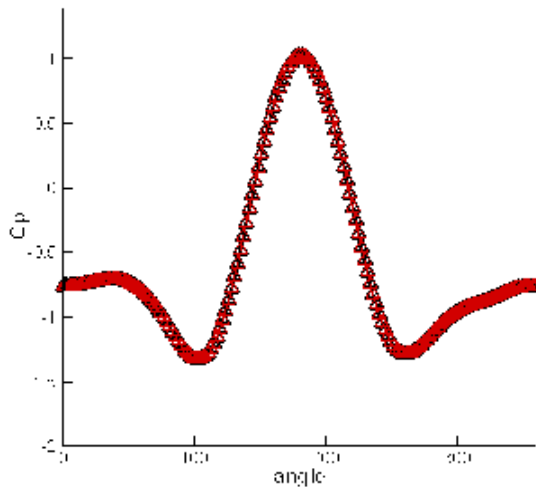
Re=20



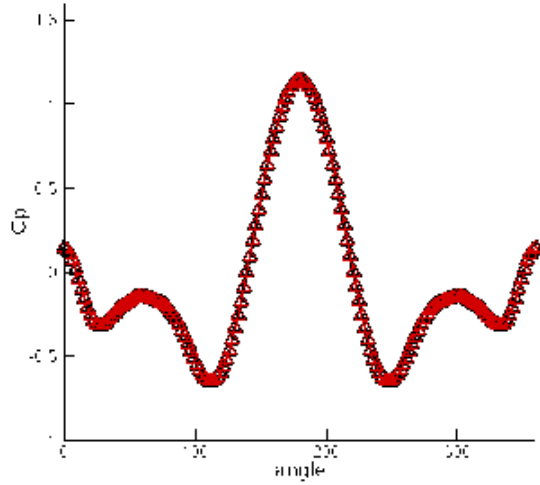
Re=40



Re=100



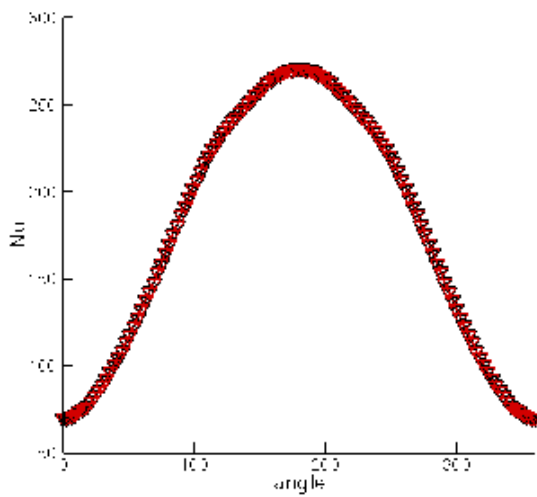
Re=160



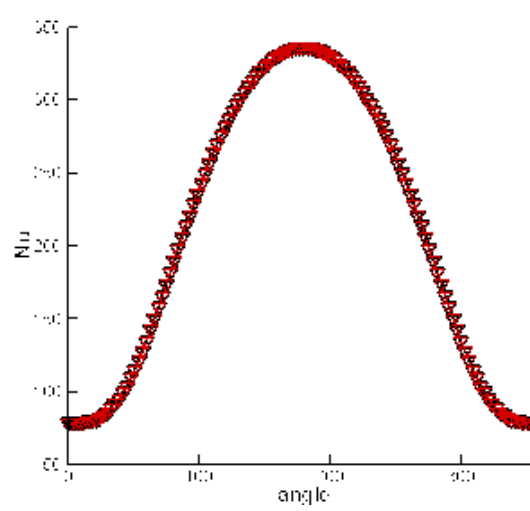
Re=1000

### 3.5 Nusselt number along the cylinder

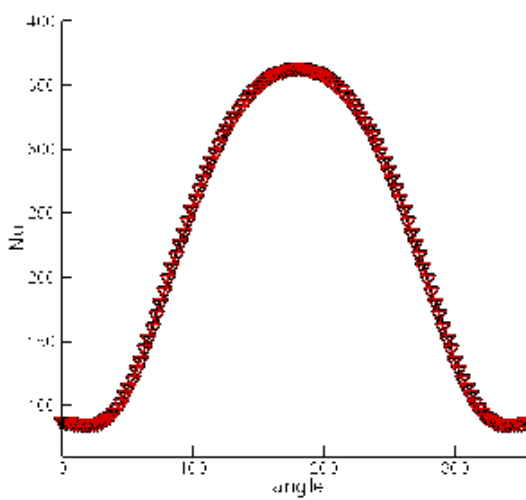
The Nusselt number is defined as  $Nu = -\frac{\partial T}{\partial n}$ .



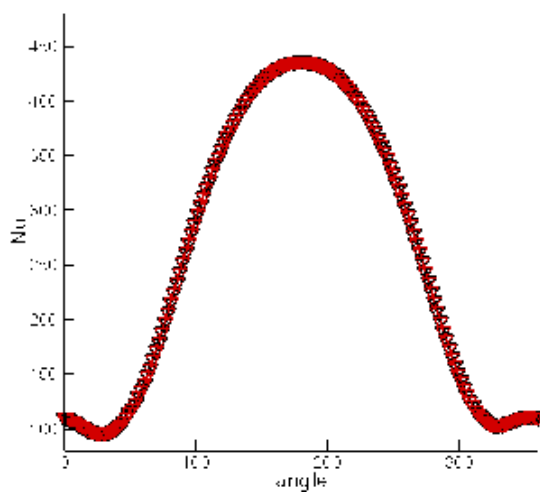
Re=4



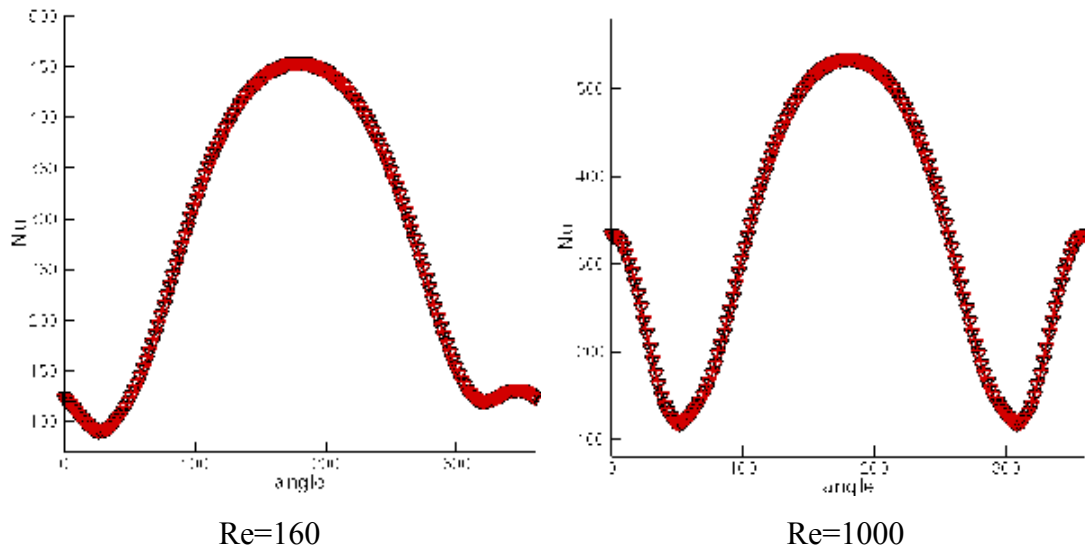
Re=20



Re=40



Re=100



Here, we define the zero angle at rear point of cylinder, and angle increases along the anti-clockwise direction. The above diagrams show variation of the average cylinder Nusselt number. The front surface consistently displays the highest Nusselt number, the top and bottom surface value is intermediate, followed by the rear surface. The rear Nusselt number is more strongly dependent on the Reynolds number in the unsteady periodic flow as compared to the steady flow regime.

#### 4. Conclusions

This study focuses on the unconfined flow and heat transfer characteristic a round cylinder in the two dimensions. The flow for  $Re \leq 40$  is noted to be steady, while that for  $Re \geq 50$  is periodic, with the transition to unsteadiness occurring between  $Re=40$  and  $Re=50$ . This agrees with prior experimental and computational studies.

The primary focus of this study, however, has been the heat transfer from the cylinder by LBM, which has not been extensively studied previously. The cylinder average Nusselt number increases with increasing Reynolds number. Finally, heat transfer correlations applicable in 2-D flow regime have been proposed for both the temperature boundary conditions considered.

The Lattice Boltzmann method is an efficient approach for the computational fluid dynamics. The major advantage of this method is that its governing equation is very simple, and it is also easy to implement by programming. In order to solve the problem of heat transfer, only the macroscopic energy equation is included. From the

above illustration we find that, using LBM along with the energy equation gives satisfactory results.

## Reference

1. S. Chen and G. D. Doolen, "Lattice Boltzmann Method for Fluid Flows", *Annu. Rev. Fluid Mech*, 1998(30), pp329-364.
2. C. Shu, X. D. Niu and Y. T. Chew, "Taylor-series Expansion and Least Squares-based Lattice Boltzmann Method: Two-Dimensional Formulation and Its Applications", *Physical Review E*, 2002(65), 036708.
3. Ganesan P., Loganathan P., "Unsteady natural convective flow past a moving vertical cylinder with heat and mass transfer", *Heat Mass Transfer*, 2001(37), pp.59-65.
4. Eagles P.M., Soundalgekar V. M., "Stability of flow between two rotating cylinders in the presence of a constant heat flux at the outer cylinder and radial temperature gradient - wide gap problem", *Heat Mass Transfer*, 1997(33), pp.257-260.
5. Armouzi M. El., Chesneau X., Zeghmami B., "Numerical study of evaporation by mixed convection of a binary liquid film flowing down the wall of two coaxial cylinders", *Heat Mass Transfer*, 2005( 41), pp.375 - 386.
6. Eswaran V., Sharma A, "Heat and fluid flow across a square cylinder in the two-dimensional laminar flow regime", *Numerical Heat Transfer*, 2004(45), pp.247-269.
7. Lange C.F., Durst F., M. Breuer, "Momentum and Heat Transfer from Cylinders in Laminar Crossflow at  $10^{-4} < Re < 200$ ", *Int. J. Heat Mass Transfer*, 1998(41), pp.3409-3430.
8. Kawamura T, Kuwahara K, "Computation of High Reynolds Numbers Flow around a Circular Cylinder with Surface Roughness. *AIAA*, 1984, pp.84-340.